

Infrared Microspectrometric Study of the Thermal History of Fusion Welding of Polyethylene

D. GUEUGNAUT, P. WACKERNIE, *Direction des Etudes et Techniques Nouvelles du Gaz de France, Centre d'Etudes et de Recherches sur les Sciences et Techniques Appliquées, 361 avenue du Président Wilson, 93210 La Plaine Saint Denis*, and J. P. FORGERIT, *Laboratoire de Spectrochimie Infrarouge et Raman (LASIR), CNRS, 2 rue Henri Dunant, 94320 Thiais, France*

Synopsis

Thermal history of a polyethylene-welded assembly has been determined by measuring the crystallinity via absorbance ratio (R_{OD}) measurements. Fourier transform infrared microspectrometry has been used because it allows a space-localized analysis within a diameter of 200 μm . A linear relation between R_{OD} and local crystallinity has been obtained using reference samples for calibration. Samples were calibrated by differential thermal analysis and density measurements. This relationship and the simulation of the various thermal treatments by calorimetric analysis allow us to characterize the different phases of the thermal history during the welding experiment.

INTRODUCTION

The structure of semicrystalline polyethylene is well known.^{1,2} The polymerization procedure can lead to different structures. The polymer consists of a crystalline fraction (the rigid fraction) buried in an amorphous material (rubberized fraction). In the crystalline fraction, which gives the material its rigidity, the macromolecules can show different arrangements: lamellar or spherulitic. The crystallinity degree or ratio χ_C measures the crystallized phase proportion of the core of the material. This parameter is very sensitive to mechanical and thermal stresses generated during the molding. This χ_C ratio can thus be related to the thermal history of polyethylene.

It is possible to study the thermal history of two pieces of polyethylene welded by fusion. To describe thermal history on each side of the welded parts, it is first necessary to draw a map of the crystallinity of the area, and then to simulate the various thermal treatments which lead to these crystalline states. The crystallinity map shows localized crystallinity gradients. The direct measure by classic "global" methods such as X-ray diffraction, calorimetric analysis, or infrared spectrometry are limited by the volume of sample examined. The development of infrared microspectrometry offers the possibility of measuring these maps for macroscopic part with excellent spatial resolution. It gives an indirect measure of the crystallinity which has to be standardized by methods such as differential thermal analysis or density measurements.

The simulation of various thermal treatments of polyethylene by differential thermal analysis offers the possibility of establishing a relationship between the crystallinity ratio and two parameters: maximum temperature reached before cooling and cooling rate.

TECHNIQUE AND EQUIPMENT

Methodology

There have been a large number of studies of crystallinity of polyethylene by infrared spectrometry. Certain absorption bands between 850 and 1400 cm^{-1} have been more especially studied: bands at 908, 1303, 1352, and 1368 cm^{-1} .³⁻⁶ In this study only the absorbance variations of bands at 908, 1303, and 1368 cm^{-1} are considered (see Fig. 1).

The absorption band at 908 cm^{-1} is related to the wagging of terminal vinyl groups ($-\text{CH}=\text{CH}_2$) located in the molecular chain plane. Their intensity strongly depends on the polymerization process used. The intensity of this absorption band is not dependent upon the crystalline state for bulk crystallized samples, but only upon the thickness of the analyzed sample and the global concentration of vinyl groups ($-\text{CH}=\text{CH}_2$). Thus, the absorption band can be used as a reference.

The absorption bands at 1303 and 1368 cm^{-1} characterize the methylene groups ($-\text{CH}_2-$) in the amorphous fraction. They are assigned to the torsion and rocking motion of the methylene groups out of the molecular chain plane.

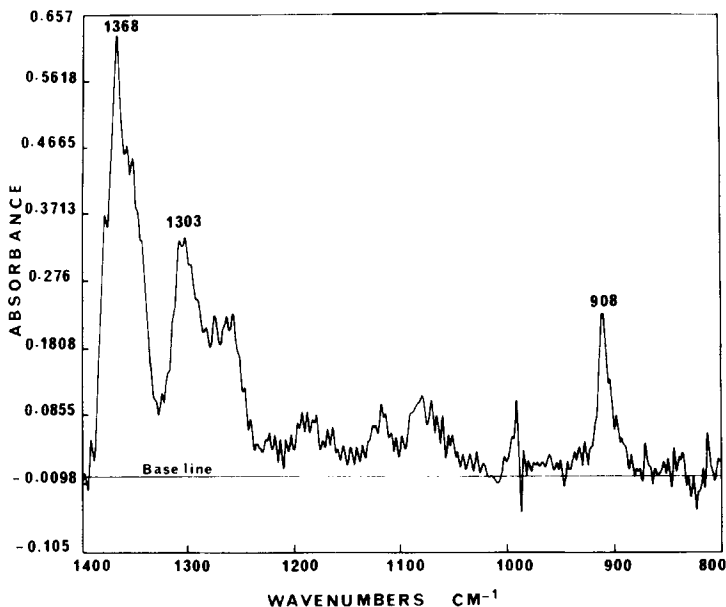


Fig. 1. Infrared spectrum of a 300 μm thick PE slice obtained by microspectrometry: characteristic bands of absorption are between 800 and 1400 cm^{-1} .

The absorbance of those bands increases when the crystallinity ratio decreases. According to Beer-Lambert law:

$$(\text{OD})_{\sigma} = \epsilon_{\sigma} \cdot b \cdot C \quad (1)$$

where $(\text{OD})_{\sigma}$ is the absorbance at the wavenumber σ , ϵ_{σ} is the absorptivity at the wavenumber σ , C is the concentration of chemical species studied (in mol. cm^{-3}), and b the thickness of the sample (pathlength, in cm).

Thus, we have:

$$\text{OD}_{908} = \epsilon_{908} \cdot b \cdot C_{\text{vinyl groups}} \quad (2)$$

$$\text{OD}_{1303} = \epsilon_{1303} \cdot b \cdot C_{\text{methylene groups}} \quad (3)$$

and

$$\frac{\text{OD}_{1303}}{\text{OD}_{908}} = R_{\text{OD} \frac{1303}{908}} = \frac{\epsilon_{1303} C_{\text{methylene groups}}}{\epsilon_{908} C_{\text{vinyl groups}}} \quad (4)$$

Where ϵ_{1303} , ϵ_{908} , and $C_{\text{vinyl groups}}$ are constants for a given polyethylene sample.

$$R_{\text{OD} \frac{1303}{908}} = K \cdot C_{\text{methylene groups}} \quad (5)$$

A similar relation is obtained for $\sigma = 1368 \text{ cm}^{-1}$ instead of 1303 cm^{-1} .

As seen above, the ratio R_{OD} in Eq. (5) is proportional to the crystallinity ratio. This method allows us to remove the thickness fluctuations, since Eq. (5) is independent of b .

Measurement of Absorbance Ratio

The large throughput and multiplex advantages made the two-wave interferometers particularly adapted to infrared microspectrometry. For this reason, an infrared microscope, Perkin-Elmer model 85, was assembled with a Fourier transform infrared (FTIR) spectrometer, Bruker 113V.

The IR part of the optical setup is composed of mirrors only. An eyepiece is used to visualize the analyzed sample area. This objective has been designed to obtain the best performances in the infrared spectral region. It is corrected for chromatic and distortion aberrations.

The mirror M_1 (see Fig. 2) placed in the sample chamber of the interferometer reflects the infrared beam in the direction of condenser C_1 which focuses the beam in S_1 . The dimensions of the focal image are $600 \times 200 \mu\text{m}$. Mirror M_2 can rotate around a vertical axis. The two-position mirror M_2 (Fig. 2) reflects the beam through the condenser C_2 which focuses the beam onto the

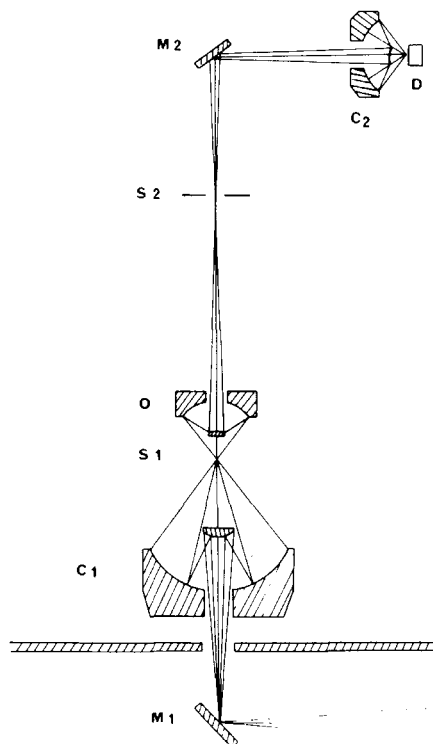


Fig. 2. Optical components of the experimental setup: Condenser C_1 and objective O (both Schwarzschild type) have the same characteristics: numerical aperture 0.75, obscuration ratio 0.41, energy loss ratio 16.8%, except for linear magnification which is 0.12 for the former and 25 for the latter. Condenser C_2 is a Cassegrain condenser type.

detector D . When M_2 is rotated by 90° , the beam is reflected to an eyepiece of $7\times$ magnification. For this last position of M_2 , the sample can be viewed through the eyepiece. The total magnification of the microscope is $175\times$.

Each spectrum was obtained with 500 scans. The spectral resolution was 4 cm^{-1} . Spectra were computed in terms of absorbance. The stability of the spectrometer was checked by comparison of two reference spectra scanned at the beginning and at the end of the experiment.

Under chosen conditions, R_{OD} ratios have an accuracy better than 3%. Absorbance for bands at 1368 , 1303 , and 908 cm^{-1} was obtained after baseline correction at 1400 , 950 , and 800 cm^{-1} .

We have designed a mechanical setup for handling the sample under the microscope. In order to minimize the deformations of the sample (thin sheet of $\sim 300\text{ }\mu\text{m}$) at the focus point of the microscope, this sample was firmly tightened between two cardboard parts with a hole in the center. The absence of a KBr disc decreases energy losses and improves the signal-to-noise ratio. The sample was fixed on the mechanical assembly (see Fig. 3). The height was adjusted with an elevator (Microcontrôle EL80, F91005 Evry, France). The horizontal micrometric displacement was equipped with a step-to-step motor (Microcontrôle UT100PP).

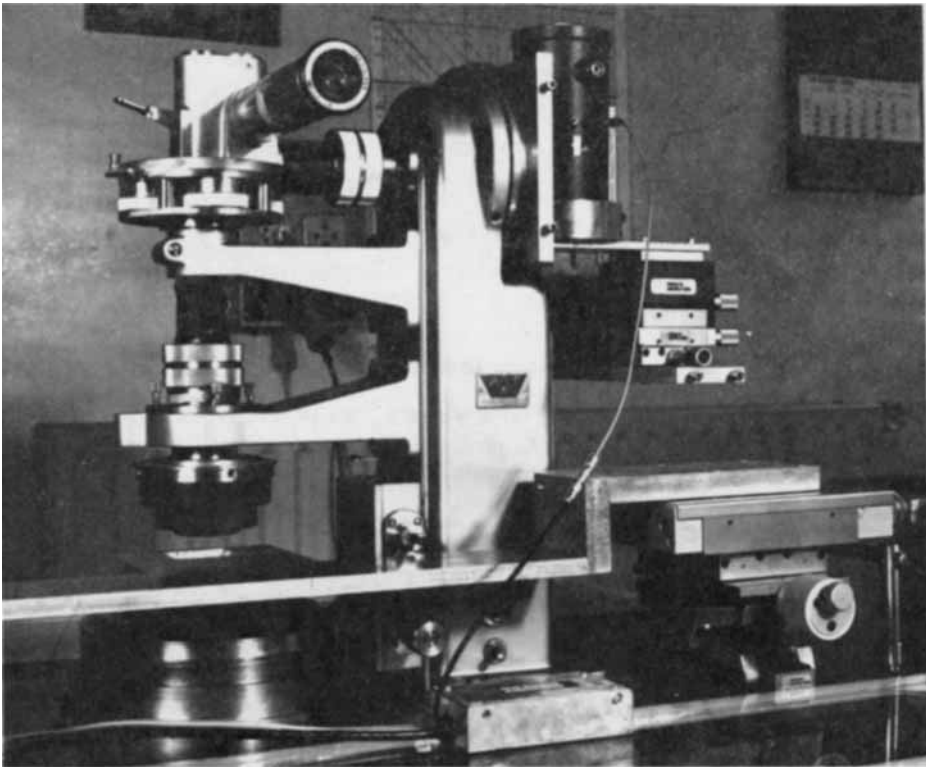


Fig. 3. Experimental setup.

Determination of Crystallinity by Differential Thermal Analysis and by Density Measurements

Polyethylene crystallinity has been obtained by two different methods: differential scanning calorimetry (DSC) and a density gradient column.

The DSC used was a Mettler DSC 30. The amount of sample was about 10 mg. The sample was melted and heated to 180°C under nitrogen atmosphere to prevent oxidation. The heating rate was 10°C/min. Numerical integration of the thermogram above a linear base chosen between 20° and 160°C leads to a computed value of the melting enthalpy ΔH^m . This value in relation with that of a totally crystallized polyethylene $(\Delta H^m)_{100\%} = 293\text{J/g}$ allowed one to obtain the crystallinity ratio χ_C ⁷ where:

$$\chi_C(\%) = \frac{\Delta H^m}{(\Delta H^m)_{100\%}} \quad (6)$$

The density was determined by the gradient column method with a two-column Davenport setup. The solutions used were mixtures of water and ethanol at 23°C. The specific gravity scale was adjusted between 0.920 and 0.970 g/cm³.

The samples studied were immersed in the solution, and after stabilization the measured value of the density ρ led to the crystallinity ratio χ_C according to the expression^{2,8}

$$\chi_C(\%) = \frac{\rho - \rho_a}{\rho_c - \rho_a} \quad (7)$$

where $\rho_a = 0.855 \text{ g/cm}^3$ and $\rho_c = 1.000 \text{ g/cm}^3$ were the densities of amorphous and crystalline polyethylene, respectively. The relative accuracy on χ_C was the same as that of ρ .

Sample Studied

Experiments were conducted on a commercial polyethylene resin Rigidex PC00240 manufactured by BP Chemicals, Grangemouth Stirlingshire, Great Britain ($\rho = 0.943 \text{ g/cm}^3$, molecular weight $\bar{M}_n \sim 15600$, polydispersity about 9.1).

Absorbance measurements by infrared microspectrometry were performed with a particular test piece (Fig. 4). It was composed of two-half pieces (Pieces 1 and 2) injected with the Rigidex resin. Before welding, pieces 1 and 2 were annealed for about 750 h in water at 80°C . Thus, their crystalline morphology was homogenized and their crystallinity increased.

Two such pieces were welded through local melting. A heating element (a $600 \mu\text{m}$ diameter wire) included in one of the pieces gave the amount of heat necessary for melting. The sample was cut perpendicularly to the junction interface (parallel to Z-axis). The slice, $300 \mu\text{m}$ thick, was obtained with a

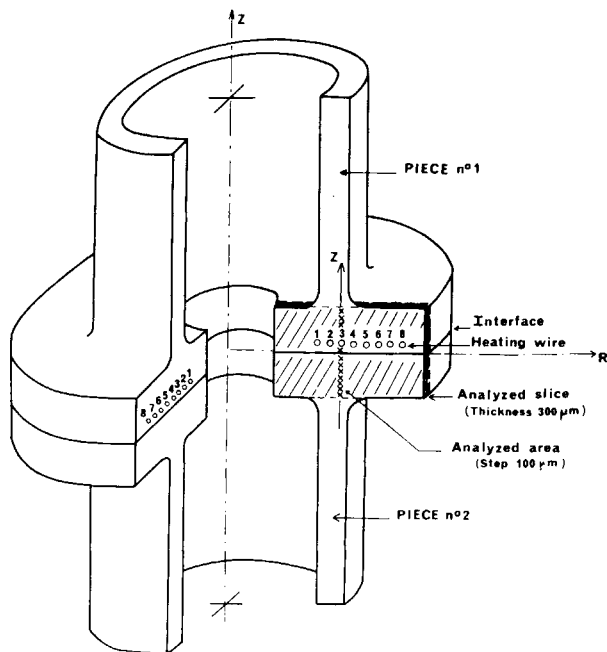


Fig. 4. Test piece (after welding) showing analyzed sample.

microtome. The thickness accuracy was better than 10%. The slice was then tightened between cardboards and positioned on the moving plate. Measurements of R_{OD} were made in front of the heating element 3, perpendicularly to interface (see Fig. 4).

Standard samples were discs of 4000 μm diameter and 350 μm thickness which were obtained from the "foot" of the welded pieces at a distance of about 15 mm from the welded interface (see Fig. 4).

The reference samples were melted and heated to 180°C under nitrogen atmosphere and immediately cooled with five different rates. The corresponding R_{OD} were measured by infrared spectrometry. Crystallinity was determined either during a second fusion by DSC according to Eq. (6), or by a density measurement according to Eq. (7).

The two parameters which were used for the thermal history simulation were the final temperature reached before cooling T_u , and the cooling rate dT/dt . Both were obtained by DSC. Samples used for simulation were heated to different T_u , then immediately cooled with 0.1°C/min to 50°C/min rates. About 30 combinations of (T_u , dT/dt) were investigated. The corresponding crystallinity was calculated from the second fusion thermograms, as described before.

RESULTS AND DISCUSSION

Crystallinity Map

Figure 5 shows the R_{OD} results for the 1303 and 908 cm^{-1} bands versus the distance from the welded junction. The zero of the scale (in μm) represents the interface. Measurements were made in Z-axis direction, on each side of the heating element located between +400 and +1000 μm .

R_{OD} is equal to about 1.01 far from the interface. Approaching the interface, R_{OD} first increases weakly up to about $-1000 \mu\text{m}$ (piece 2) and $+2500$

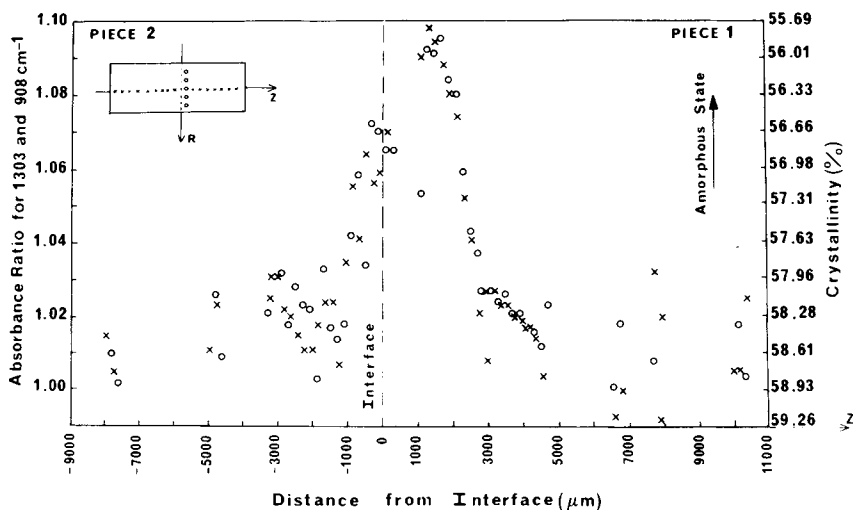


Fig. 5. Absorbance ratio for 1303 and 908 cm^{-1} bands (left scale) and crystallinity (right scale) versus distance from interface.

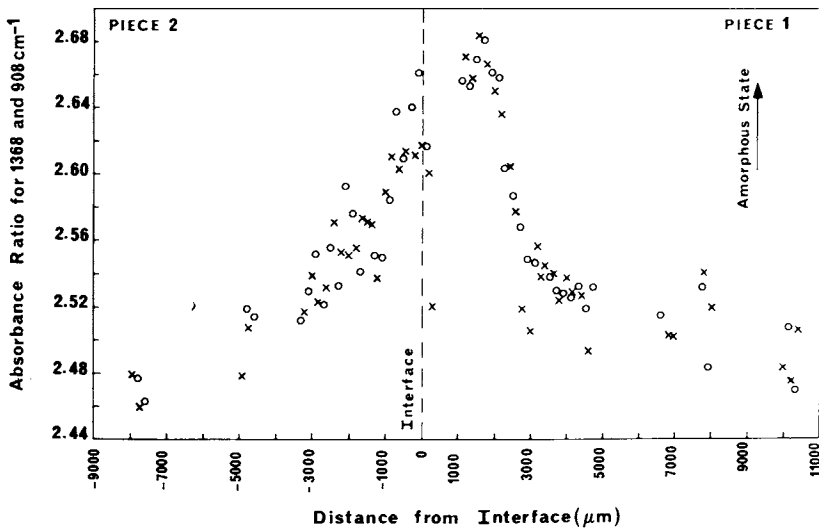


Fig. 6. Absorbance ratio for 1368 and 908 cm^{-1} bands versus distance from interface.

μm (piece 1), and then increases sharply and reaches two maximum values, 1.07 and 1.10, located at -100 and $+1500 \mu\text{m}$, respectively, one of them being consequently very close to the interface (0 of the scale).

As shown before, attained crystallinity decreases when approaching the interface.

The same phenomenon is observed with the R_{OD} results for 1368 and 908 cm^{-1} bands (see Fig. 6). The position of the two maxima are the same ($R_{\text{OD}} = 2.65$ and 2.68). However, the profile is less precise in piece 2. The 1368 cm^{-1} absorption band leads to a loss of accuracy in the determination of the crystallinity because it is influenced by the neighborhood of the 1378 cm^{-1} absorption band.

Proportionality between R_{OD} and χ_C must be measured to express results of Figure 5 in terms of crystallinity. This relation was established with standard samples, as previously explained. Figure 7 shows the linear regression, with a correlation coefficient of -0.985 , which contains five experimental points. The proposed relation is the following:

$$R_{\text{OD}} = -0.0308\chi_C + 2.8148 \quad (8)$$

The behavior of the crystallinity χ_C versus the distance from the interface can be interpolated from Eq. (8). χ_C remains between two limits of crystallinity that are 55.7% and 59.3%. Under these conditions, the overall crystallinity variation from one part to the other of the welded piece is close to 3.6%. Crystallinity values are reported on the right scale of the Figure 5.

Variations of χ_C versus distance from the interface represent the crystallinity changes inside the material under the thermal conditions of the welding treatment. Nevertheless, several combinations of (T_u , dT/dt) can lead to the same value of χ_C . The simulation of different thermal histories were thus necessary.

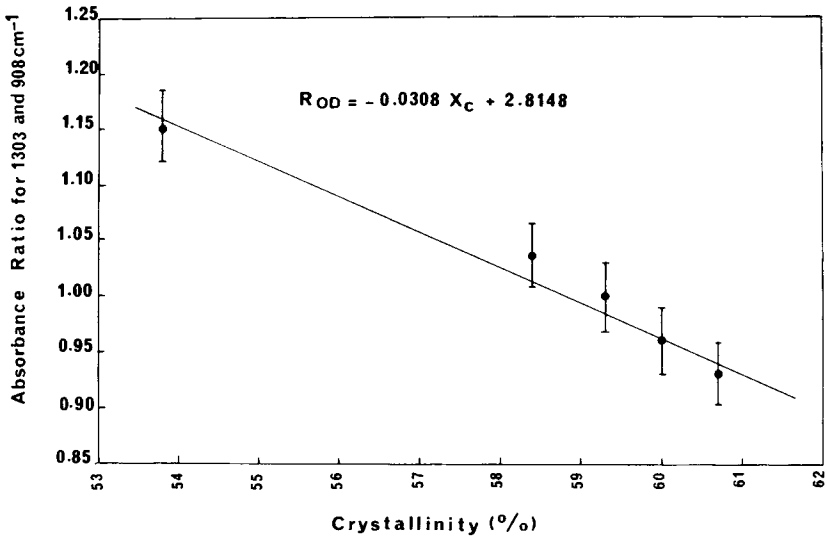


Fig. 7. Crystallinity versus absorbance ratio for 1303 and 908 cm^{-1} bands. $R_{OD} = -0.0308\chi_C + 2.8148$.

Analysis of the Polyethylene Thermal History During the Welding Process

Thermal history simulation on standard samples. Figures 8 and 9 show the behavior of χ_C versus maximum temperature T_u for different cooling rates dT/dt . The melting temperature T_m about 125°C (peak of the thermogram) represents the limit between two domains in which polyethylene behaves differently.

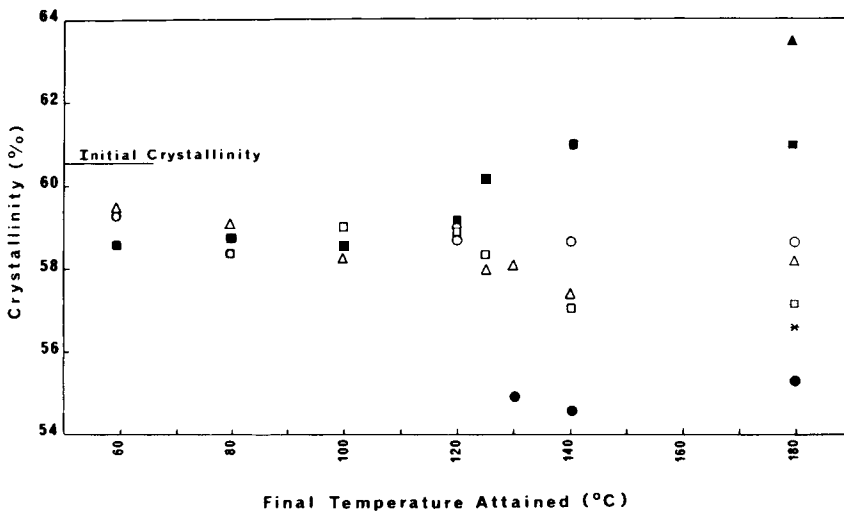


Fig. 8. Final temperature dependence of crystallinity for different cooling rates: (▲) 0.1°C/min; (■) 2°C/min; (○) 5°C/min; (△) 10°C/min; (□) 20°C/min; (*) 30°C/min; and (●) 50°C/min.

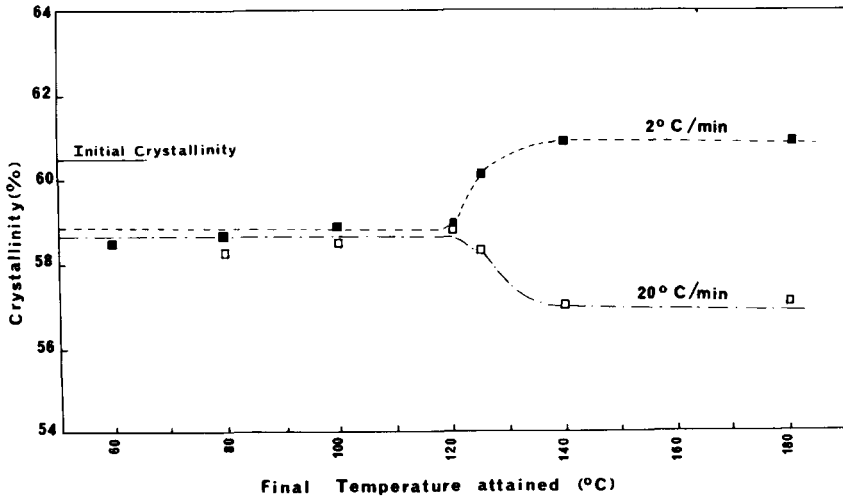


Fig. 9. Final temperature dependence of crystallinity for cooling rates of 2°C/min (■) and 20°C/min (□).

Beyond T_m the more complete the fusion is, the greater the dependence between χ_C and dT/dt . The complete fusion occurs at about 140°C. For T greater than 140°C, the thermal history of annealing vanishes completely. Final crystallinity only depends on the cooling rate: χ_C decreases when increasing dT/dt . Thus, the polyethylene structure becomes more amorphous. Variations of χ_C versus dT/dt from the melt (180°C) are shown in Figure 10. χ_C can be determined by:

$$1 - \chi_C = \exp \left[-0.938 \left(\frac{dT}{dt} \right)^{-0.03} \right] \quad (9)$$

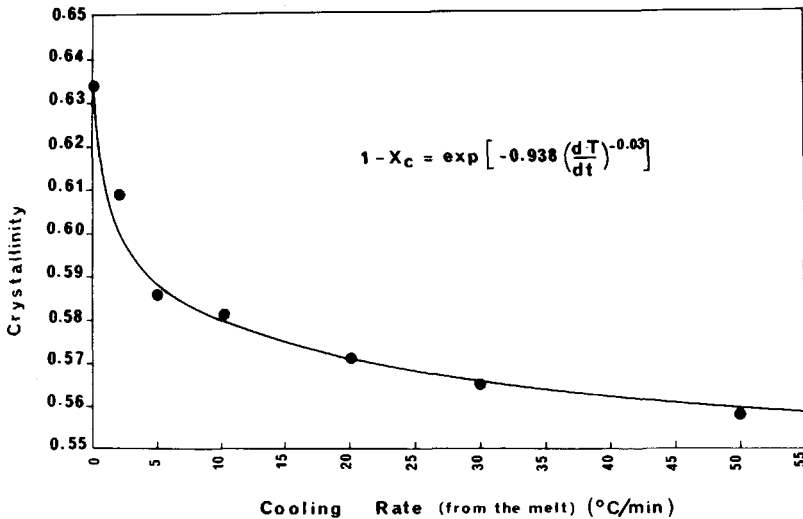


Fig. 10. Cooling rate dependence of crystallinity from the melt (180°C). $1 - \chi_C = \exp[-0.938(\frac{dT}{dt})^{-0.03}]$.

This relation is very close to that proposed by Avrami⁹ in the case of an isothermal crystallization:

$$1 - \chi_C = \exp(-At^n) \quad (10)$$

where A is a rate constant, t the crystallization time at a given temperature T , and n a dimensional factor which varies between 1 and 4 for a given nucleation-growth mechanism. Eq. (9) cannot be obtained directly from Eq. (10), and the similarity with Eq. (9) proposed by Ozawa¹⁰ and derived from Eq. (10) does not appear to be transposable to the polyethylene studied.

For temperatures lower than T_m , the final crystallinity varies weakly with cooling rate. The mean value is close to 58.5 or 59% and lower than initial crystallinity (about 60.5%) for the cooling rate investigated.

Thermal history analysis of the welded sample. As shown in Figure 8, χ_C varies between 63 and 55% for the different cooling rates. This gradient of 8% is greater than that on the welded sample (3.6%) (see Fig. 5). From the preceding measurements, the thermal history of the welded sample can be determined.

The sharp decrease down to a value of χ_C lower than 58.5% between -1000 and $+2500 \mu\text{m}$ corresponds to the melting of polyethylene at a temperature higher than T_m followed by a cooling with a rate greater than $5^\circ\text{C}/\text{min}$. The minimum values of χ_C (56.7 and 55.7%) at -100 (piece 2) and $+1500 \mu\text{m}$ (piece 1) correspond to the maximum values of the cooling rate. Maximum values of dT/dt at these distances are, respectively, equal to or higher than $20^\circ\text{C}/\text{min}$ and $40^\circ\text{C}/\text{min}$. The difference of those minimum values of χ_C from piece 1 to piece 2 is explained by a greater cooling rate in piece 1. This difference may be caused by the physical discontinuity at the interface before welding. The melting point defines an area where the polyethylene reaches temperatures higher than 125°C during welding. It can be localized between -1000 and $+2500 \mu\text{m}$. With a size of about $3500 \mu\text{m}$, this area is weakly disymmetrical and greater in piece 1 where the heating element is located. Optical microscopy shows a similar phenomenon.

Out of this molten area, crystallinity increases sharply to a value close to 58.5% indicating a zone where the polyethylene has been heated at temperatures below T_m .

CONCLUSION

Infrared microspectrometry is well adapted to localized crystallinity measurements on a macroscopic polyethylene sample. With this method, the thermal history of two fusion-welded pieces can be attained. Nevertheless, uncertainties in the measurements do not allow one to estimate weak crystallinity gradients. In addition, better homogenization of the structure of the pieces before welding could lead to more accuracy in determining the thermal history after welding.

References

1. *Groupe Français d'Etudes et d'Applications des Polymères*, Vol. 4, CNRS-CERMAV, Saint Martin d'Hères, 1982.
2. C. Reckinger, F. C. Larbi, and J. Rault, *J. Macromol. Sci. Phys.*, **B23**, 511 (1985).

3. T. Okada and L. Mandelkern, *J. Polym. Sci.*, A-2, **5**, 239 (1967).
4. T. Okada and L. Mandelkern, *Polym. Letters*, **4**, 1043 (1966).
5. W. Glenz and A. Peterlin, *J. Macromol. Sci. Phys.*, **B4**, 473 (1970).
6. P. J. Miller and J. F. Jackson, *J. Polym. Sci. Polym. Phys. Ed.*, **11**, 2001 (1973).
7. G. Champetier and L. Monnerie, *Introduction à la Chimie Macromoléculaire*, Masson & Cie, Paris, 1969.
8. R. Seguela and F. Rietsch, *Polymer*, **27**, 532 (1986).
9. *Groupe Français d'Etudes et d'Applications des Polymères*, Vol. 1, CNRS-CERMAV, Saint Martin d'Hères, 1982.
10. T. Ozawa, in *Thermal Analysis: Comparative Studies on Materials*, edited by H. Kambe and P. D. Garn, Halsted Press, Tokyo, 1974, p. 155.

Received May 7, 1987

Accepted August 20, 1987